

# Comparison of TRM and FRP in Torsional Strengthening of RC Beams Using Glass Fibers Under Repeated Loads

Hudhaifa F. Ismael, Saad M. Raof, Muyasser M. Jomaah

*Department of Civil Engineering, University of Tikrit, Tikrit, Iraq  
E-mails : hudhaifa.f.ismael@tu.edu.iq*

This article investigates the effectiveness of TRM and FRP in torsional strengthening of RC beams under repeated loads. The examined variables were: the type of strengthening system (TRM versus FRP), the strengthening configurations (partially & fully) and the strengthening orientation ( $45^\circ$  &  $90^\circ$ ). seven full-scale beams were casted, strengthened, and tested repeatedly up to failure. One used as a control, three specimens were strengthened with TRM and the rest three specimen were retrofitted with FRP. It was mainly found that: (a) the effectiveness of TRM composites in increasing the torsional capacity was approximately similar to that of FRP composites; (b) The partially strengthening configurations was more effective in increasing the torsional capacity than the fully strengthening configurations in both strengthening systems (TRM & FRP); (c) The  $90^\circ$  strengthening orientation was more effective in enhancing the torsional capacity than the  $45^\circ$  strengthening orientation in both strengthening system (TRM & FRP).

**Keywords:** TRM, FRP, Glass fibres, Repeated load, Torsional strengthening.

## 1. Introduction

The RC beams in multi-story parking garages, ports, bridges, and airport facilities may be subjected to repeated loads. Due to the continuous process of loading and unloading, environmental degradation, ageing, and Lack of maintenance, rustled to structurally deficiencies may occur Therefore, strengthening is considered an important issue in overcoming these challenges [1].

In last years, FRP demonstrated high superiority in external strengthening for RC torsion in comparison to other methods due to low weight, flexibility of application, corrosion resistance and high strength and stiffens, on the other hand, FRP had several drawbacks recorded in [2, 3].It is worth noting, all these drawbacks are associated to use an organic matrix (epoxy resin)[4, 5].

To alleviate these challenges, a novel composite material named Textile-Reinforced Mortar (TRM) has been developed. This composite comprised fibers in form of textile impregnated with an inorganic materials (e.g. modified cement mortar) as a bonding agent[6], The advantages of this composite material are recorded in[7, 8].

several studies in the last decades concerned with use of FRP in torsional strengthening for RC under monotonic loads[9-13]. On the other hand, only one study used FRP for torsional strengthening of RC beams under repeated loads (7 cycles of 60% of the ultimate load of the control specimen) by Tais and Abdulrahman (2023)[14]. Eight specimens were casted and strengthened by CFRP strips for different configuration 45°; one strip fully wrapped; double strip fully wrapped; and spiral strip around the sample. The main conclusions of this study were: (a) The double strip fully wrapped showed higher enhancement in torsional capacity for both monotonic and repeated loads; (b) The behavior of the specimens was identical under monotonic and repeated loads. And, (c) The torsional capacity reduced due to loading and unloading under repeated loads compared with monotonic loads[14].

The survey in the literature demonstrated that the only studies on the use of TRM for torsional strengthening under monotonic load are limited. these studies were conducted by Alabdulhady et. al. (2017) and Al-Abdulhadi and Sneed (2018)[3, 15]. In particular, the study conducted in [15] examined the torsional characteristics of rectangular beams that were strengthened using PBO-TRM. Five beams were created, strengthened, and subjected to torsional testing under a monotonic load. The parameter under consideration was the configuration of strengthening (i.e. fully and partially). The fully configuration exhibited a greater enhancement in torsional capacity compared to the partially configuration. Also, Al-Abdulhadi and Sneed (2018) investigated the effect of different strengthening orientations (90° and 45°), strengthening configurations (fully and partially), and the number of strengthening layers (one and two) on torsional strength. PBO-TRM was used to strengthen ten rectangular RC beams. They concluded that the 90° strengthening orientation was better than the 45° strengthening orientation, and increasing the number of layers significantly improved the torsional capacity [3].

It is clear that the available literature does not cover adequately the subject of strengthening of RC beams in torsion under repeated loads using TRM did not covered yet. In particular, the effectiveness of TRM versus FRP in torsional strengthening due to the significance of repeated loading as they apply to numerous loading scenarios in practice, including the passage of vehicles on bridges, offshore loading, pedestrian loads, machine loads, and seismic loading. Therefore, the current study, provides for the first-time a comprehensive comparison of TRM versus FRP for strengthening of full-scale RC beams by glass fibers in torsional under repeated loads. Taking into account variety of variables, namely; (a) strengthening configurations (fully & partially) and (b) strengthening orientation (90° & 45°).

## **2. Experimental program**

### **2.1. Test specimens and investigated parameters**

This study aimed to assess the performance of TRM versus FRP in torsional strength of full-scale RC beams when subjected to repeated loads. For this goal, seven full-scale rectangular

beams were fabricated and cast, with a total length of 3000 mm, whereas the clear torsional span was 2200-mm and cross-section of 150 mm width and 250 mm high (Fig. 1). The longitudinal reinforcement ratio ( $\rho_{sl}$ ) was 1.52% whereas, the transverse reinforcement ( $\rho_{st}$ ) was 0.4% ACI 318 code [16], where:

Asl: Total longitudinal bar area ( $\rho_{sl} = Asl/Ac$ )

Ac: Concrete area gross ( $A_c = b \times h$ )

Ast: One stirrup leg area ( $\rho_{st} = Ast/Ac \cdot pt/s$ )

pt: Stirrup perimeter

S: Stirrup spacing (center-to-center).

Dimensions and details of the RC beams are shown in (Fig. 1).

A higher shear reinforcement ratio ( $\rho_{st} = 0.8\%$ ) was provided under the clamps to prevent the local failure due to stress concentration as shown in Fig. 1. Deformed steel bars with diameters of (10 mm) and (8 mm) were used as longitudinal reinforcement, whereas, deformed steel bars with diameter of (8 mm) were used for closed stirrups (see Fig. 1). A tensile test was conducted to evaluate the mechanical properties in accordance with [17]. The results of the test are presented in Table 1.

Table 1. Tensile properties of steel reinforcement

Material
Yield strength, (MPa)
Ultimate strength, (MPa)

The investigated variables were: (a) strengthening system (TRM vs. FRP) (b) the strengthening configurations (fully & partially) and (c) strengthening orientation ( $90^\circ$  &  $45^\circ$ ).

The notation of the strengthened specimens follows X $\theta$ -G-Z-T where X: type of strengthening system (TRM or FRP),  $\theta$ : strengthening orientation ( $\theta = 45^\circ$ , or  $90^\circ$ ) with relation to the beam's longitudinal axis, G: glass fiber material, Z: the strengthening configurations (P for partially and F for fully) and T: loading type (M for monotonic and R for repeated).

One specimen was un-strengthened as a control, whereas, the other six specimens were strengthened as shown in Fig. 2 shows. All strengthened specimens were wrapped in a 3-sides U-jacket shape (Fig. 2). U-jacket configuration was adopted because in real applications, the closed jacket of the beam may not be available for strengthening, similar to a T-beam in a monolithic building.

## 2.2 Materials properties

The concrete compressive and splitting tensile strength were measured using average results of three cylinders with dimensions of  $150 \times 300$  mm. The test was performed on the testing day, following the guidelines set by ASTM C39&C496 [18, 19]. The modulus of rupture was also evaluated using prisms with dimensions of ( $100 \times 100 \times 500$  mm) according to ASTM C78 [20]. The mechanical properties of the concrete are listed in Table 2.

Table 2. Measured concrete properties.

Material	Concrete
Compressive strength, (MPa)	25
Splitting tensile strength, (MPa)	2.34
Modulus of rupture (MPa)	3.24

A coated glass fiber textile (PTFE glass) were used for strengthening. The textile weight, mesh size, and thickness are listed in Table 3. A uniaxial tensile test was performed on TRM coupons to evaluate mechanical characteristics of the composite. Fig. 3a shows the coupon's geometric properties, whereas Fig. 3b illustrates the setup process, and Fig. 3c shows the coupon failure mode. Table 4 displays the value of ultimate stress ( $f_{fu}$ ) of TRM coupons (average of three specimens).

Table 3. Details of the textiles according to the manufacturer datasheets

PTFE coated glass textile

Thickness(mm)	0.45
Weight (g/m <sup>2</sup> )	430
Mesh size (mm)	10*10
Density (gm/cm <sup>3</sup> )	2.5
Tensile strength (Mpa)	1400
Elastic Modulus (Mpa)	-
PTFE content (%)	29

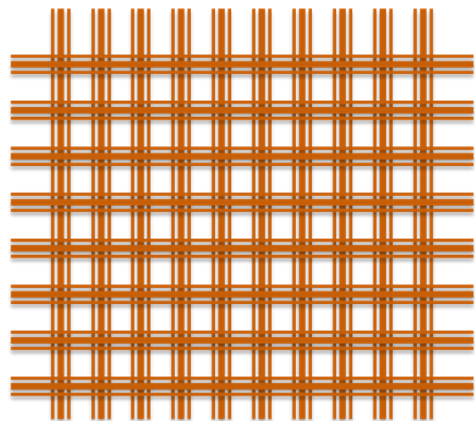


Table 4. Ultimate tensile stress ( $f_{fu}$ ) of TRM coupons

TRM Coupon	No. of layers	Ultimate tensile Strength ( $f_{fu}$ ) (MPa)
PTFE GLASS	1	1345

The TRM binding material was an inorganic modified cement mortar with a water-to-cement ratio of 0.17:1. According to ASTM C39 and C496 standards,[18, 21]. its mean compressive strength was 40 MPa, and its mean tensile strength was 3.6 MPa. For FRP strengthening, a commercial epoxy resin was used, mixed at a 4:1 ratio.

### 2.3 Technique of strengthening

The strengthening system (TRM or FRP) was applied externally according to the strengthening configuration (Fig. 2). Both strengthening techniques followed the steps described below:

A mesh of grooves (100×100mm) mm was create with a depth of 2-3 mm using grinding machine (Fig. 4a). Then, compressed air was used to clean the concrete surface.

The application of TRM materials consists of three steps: (i) Use water to wet the concrete surface, (ii) applying a layer of mortar (Fig. 4b), and (iii) carefully pressing the textile into the mortar manually to ensure an effective impregnation with cement mortar (Fig. 4c).

In FRP enhanced specimens, textile fibre was impregnated with a plastic roller over a thin resin layer (Fig. 4d).

## 2.4 Test setup

The test setup is shown in (Fig. 5a & b). In previous works[3, 22], the same test setup was adopted. A hydraulic jack with a 500-kN capacity was used to apply the torque to the specimens by a loading arm, of 700-mm eccentricity with respect to the cross-section's centroid. The loading protocol included application of load equal to 60% of the experimental ultimate load of the control specimen. The load was approximately equivalent to the maximum expected loads that beam specimens can carry at a service stage in bridge engineering applications [AASHTO specifications (AASHTO 2012)][23]. This repeated load was applied seven loops, and then the twist was increased until total failure of the specimen. The angle of rotation was measured by (LVDT) that was attached to the bottom of the beam (150 mm from the longitudinal axis) at the side of the loading arm to measure the displacement and then calculate the corresponding angle of rotation (see Fig. 5c).

## 3. Experimental results

Table 5 shows all specimen results. This Table include: (1) The cracking torque ( $T_{cr}$ ). (2) the percentage of increase of the cracking torque of strengthened specimens compared to the control. (3) The cracking angle of twist ( $\theta_{cr}$ ). (4) The ultimate torque ( $T_u$ ). (5) the percentage of increase in ultimate torque. (6) The ultimate angle of twist ( $\theta_u$ ) corresponding to the ultimate torque. (7) the increase of the ultimate angle of twist compared to the control specimen and (8) the failure mode.

Table 5. Summary of test results.

Specimens name	$T_{cr}$ (kN.m) (1)	increase in cracking torque (%) (2)	$\theta_{cr}$ (deg./m) (3)	$T_u$ (kN.m) (4)	increase in ultimate torque (%) (5)	$\theta_u$ (deg./m) (6)	$\theta_u/\theta_{u,con}$ (7)	Failure mode* (8)
CON-M <sup>1</sup>	5.6	-	3.05	7.42	-	7.9	-	CC
CON-R	4.97	0.88	1.99	6.70	0.9	4.86	0.62	CC
<b>TRM-retrofitted</b>								
T <sub>90</sub> -G-F-R	7	41	2.48	8.4	25	8	1.65	DR
T <sub>90</sub> -G-P-R	6.23	25	1.64	8.8	31	4.57	0.94	RC
T <sub>45</sub> -G-P-R	6	21	1.85	7	4	7.5	1.54	RC
<b>FRP-retrofitted</b>								
F <sub>90</sub> -G-F-R	9.8	97	3.05	10.85	62	4.95	1.02	DR

F <sub>90</sub> -G-P-R	9.58	93	2.67	11.2	67	4.95	1.02	RC
F <sub>45</sub> -G-P-R	9	81	2.14	9.6	43	3.05	0.63	RC

\* CC: Concrete crushing; RC: fiber rupture accompanied by concrete crushing; DR: deboned from the concrete substrate with rapture of fibers.

1 Specimen included in “TRM verses FRP in Torsional Strengthening of RC Beams “submitted as a journal paper to composite C.

### Torque-twist response

The loading level for each cycle was 60% of Tu of the corresponding specimen tested under monotonic load (Fig. 6). Since it was difficult to record all torque information such as: the angles of twist, first cracks, and torque during the whole repeated loading if applied several huge loops, therefore seven loops were adopted to control the record of data from loading. after there, the load increased until failure.

The torque-twist response for all experimental specimens under repeated loads is presented in Fig. 7. In general, torque-twist relationship all of specimens was identical comprising three stages: the first stage was un-cracked stage; the second stage: development of cracks until yielding the steel reinforcement; and the third stage: post-yielding response up to failure.

At the beginning of loading, the torque-twist curve was nearly linear, with a relatively high stiffness until first crack occur (first stage). After cracking, the behavior continued to be approximately linear, with relatively lower stiffness than un-cracking stage. This was attributed to the transfer of stresses from the concrete to the steel reinforcement. At this stage, the composite materials (TRM & FRP) were activated and increased the beam torsional resistance (second stage). Before reaching the ultimate capacity, the behavior became nonlinear with significant drop in the stiffness. Finally, the loading was terminated when the specimen capacity significantly dropped down (the beam demonstrated noticeable increase in the twist angle without any corresponding increase in the torque).

Table 6 presents the values of stiffness at the pre-cracking and cracking stages. The torsional stiffness was calculated according to [24].

### Ultimate torque

The values of peak torque of all tested specimens under repeated loads are listed in Table 5. The ultimate torque of reference specimen (Tu) was 6.7 kN.m while the corresponding angle of twist ( $\theta_u$ ) was 4.86 deg/m.

All TRM-strengthened specimens failed in torsion at loads more than the reference beam (Table 5). the failure torque achieved for beams T90-G-F-R, T90-G-P-R, and T45-G-P-R was 8.4, 8.8, and 7 kN.m. respectively. This yields contribution in the torsional strength of 25%, 31%, and 4%, respectively.

On the other hand, for FRP strengthened specimens., the failure torque for specimens F90-G-F-R, F90-G-P-R, and F45-G-P-R was 10.85, 11.2 and 9.6 kN.m. Hence, various FRP strengthening systems contributed 62%, 67%, and 43% respectively.

### failure modes

The failure modes observed for all tested beams are shown in Figs. 8&9. The control beams

demonstrated typical RC torsional behavior, with continuous helical diagonal cracks with a main angle of twist approximately  $45^\circ$  w.r.t the axis of rotation (Fig. 8a1, a2). Failure was controlled by crushing the concrete strut in one-third of the tested zone after steel yielding of the stirrups (Fig. 8a1, a2).

Depending on the strengthening configuration and materials, TRM-strengthened specimens (Fig. 8) failed in several different modes:

Beam T90-G-F-R showed peeled-off TRM composite under repeated load and failed due to the debonding of TRM from the concrete surface accompanied by rupture of fibers (Fig. 8b).

Failure mode of the specimens T90-G-P-R and T45-G-P-R was as a result of concrete crushing between struts accompanied with fiber rupture (Fig. 8c & d).

For FRP-strengthened specimens, different distinct failure modes were noticed as illustrated in Fig. 9a-c below:

F90-G-F-R failed due to the debonding of the FRP composite from the concrete surface due to repeated loads followed by concrete crushing (Fig. 9a).

The Specimens F90-G-P-R and F45-G-P-R failed due to the combination of concrete crushing and rupture of fibers (Fig. 9b&c)

## 4. Discussion

### 4.1 TRM vs FRP effectiveness

Table 7 present the effectiveness factor ( $k$ ) of TRM versus FRP. This factor was defined as the ratio of the ultimate torque of TRM strengthened specimens to the ultimate torque of the counterpart FRP strengthened specimens. This factor varied from 0.73 to 0.79 depending on the examined variables.

the effectiveness factor of specimens T90-G-F-R, T90-G-P-R and T45-G-P-R was 0.77,0.79,0.73 respectively. the higher performance of the FRP system could be attributed to better stress redistribution contrary to the TRM system in the coated glass fiber. (Fig. 10) illustrates the torsional capacity increase of TRM versus FRP.

### 4.2 Strengthening configurations

In general, the partially configuration specimens showed higher torsional capacity compared to the corresponding fully strengthened specimens (Fig. 11a). Specifically, for TRM-strengthened specimen T90-G-P-R recorded higher torsional enhancement of 1.05 times than specimen T90-G-F-R, respectively. the lower contribution of fully configuration-strengthened specimens could be attributed to abrupt jacket debonding accompanied by slippage of fibers due to repeated load (Fig. 8c&b).

Similarly, for FRP-strengthened specimen (Fig. 11a). F90-G-P-R recorded higher torsional enhancement of 1.03 times than specimen F90-G-F-R. the reason for less effectiveness for fully configuration strengthened specimens was related to the final failure mode, which was premature depending of the FRP composite from the concrete substrate due to repeated loads



accompanied by rupture of fibers (Fig. 9b&a)

### 4.3 Strengthening orientations

As shown in Fig. 2, two strengthening orientations ( $45^\circ$  &  $90^\circ$ ) were adopted. As shown in Fig.11b, for TRM-strengthened specimens, the  $90^\circ$  strengthening orientation was more effective in increasing the torsional capacity than the  $45^\circ$  strengthening orientation. In specific, specimen T90-G-P-R showed higher effectiveness of 1.26 times than T45-G-P-R. Similarly, for FRP-strengthened specimens, the specimens F90-G-P-R showed enhancement of 1.17 times than specimens F45-G-P-R, respectively.

The identical failure mode observed for strengthening orientation specimens which is related to the rupture of fibers and concrete crushing as shown in (Fig. 8c&d and, Fig. 9b&c). Repeated loads resulted in premature failure for  $45^\circ$  orientation strengthening compared to  $90^\circ$  orientation strengthening, hence reduced the torsional capacity in the  $45^\circ$  strengthening orientation.

## 5. Conclusions

This study experimentally evaluated the performance of TRM and FRP composites for torsional strengthening of RC beams subjected to repeated loads. Several factors were examined, including: (a) the type of reinforcement material (TRM vs. FRP), (b) the configurations of the strengthening, and (c) the orientation of the strengthening. The results led to the following conclusions:

TRM composite had approximately the same effectiveness compared to FRP composites in increasing the torsional capacity. However, the effectiveness varied depending on the investigated parameters.

The partially strengthening configurations was more effective in increasing the torsional capacity than the fully strengthening configurations in both strengthening systems (TRM & FRP) due to abrupt debonding for TRM& FRP composite from the concrete substrate under repeated loads, and the specimen F90-G-P-R achieved higher torsional enhancement of 67 % compared to reference specimen.

The  $90^\circ$  strengthening orientation was more effective in enhancing the torsional capacity than the  $45^\circ$  strengthening orientation in both strengthening system (TRM & FRP). Repeated loads resulted in premature failure for  $45^\circ$  orientation strengthening compared to  $90^\circ$  orientation strengthening.

For TRM- strengthened specimens, different failure modes were noted namely: fiber rupture accompanied by concrete crushing (T90-G-P-R and, T45-G-P-R), and debonding from concrete substrate accompanied with partial rupture of fibers textile (T90-G-F-R). Similarly, for FRP- strengthened specimens the observed failure mode was: concrete crushing accompanied by fiber rupture (F90-G-P-R and F45-G-P-R.), and debonding from the concrete substrate with concrete crushing (F90-G-F-R).



## References

1. Higgins, L., et al., Behaviour of cracked reinforced concrete beams under repeated and sustained load types. *Engineering structures*, 2013. 56: p. 457-465.
2. Raoof, S.M., L.N. Koutas, and D.A. Bournas, Bond between textile-reinforced mortar (TRM) and concrete substrates: Experimental investigation. *Composites Part B: Engineering*, 2016. 98: p. 350-361.
3. Alabdulhady, M.Y. and L.H. Sneed, A study of the effect of fiber orientation on the torsional behavior of RC beams strengthened with PBO-FRCM composite. *Construction and Building Materials*, 2018. 166: p. 839-854.
4. Ombres, L., Structural performances of reinforced concrete beams strengthened in shear with a cement based fiber composite material. *Composite Structures*, 2015. 122: p. 316-329.
5. Sneed, L.H., et al., Flexural behavior of RC beams strengthened with steel-FRCM composite. *Engineering Structures*, 2016. 127: p. 686-699.
6. Bournas, D.A., et al., Textile-reinforced mortar versus fiber-reinforced polymer confinement in reinforced concrete columns. *ACI Structural Journal*, 2007. 104(6): p. 740.
7. Tetta, Z.C., T.C. Triantafyllou, and D.A. Bournas, On the design of shear-strengthened RC members through the use of textile reinforced mortar overlays. *Composites Part B: Engineering*, 2018. 147: p. 178-196.
8. Raoof, S.M., Bond between textile reinforced mortar (TRM) and concrete substrate. 2017, University of Nottingham.
9. Patane, A. and G. Vesmawala, Experimental and analytical investigation of the behaviour of reinforced concrete beam under pure torsion. *Materials Today: Proceedings*, 2023.
10. Askandar, N.H., A.D. Mahmood, and R. Kurda, Behaviour of RC beams strengthened with FRP strips under combined action of torsion and bending. *European Journal of Environmental and Civil Engineering*, 2022. 26(9): p. 4263-4279.
11. Al-Bayati, G., R. Al-Mahaidi, and R. Kalfat, Experimental investigation into the use of NSM FRP to increase the torsional resistance of RC beams using epoxy resins and cement-based adhesives. *Construction and Building Materials*, 2016. 124: p. 1153-1164.
12. Elwan, S., Torsion strengthening of RC beams using CFRP (parametric study). *KSCE Journal of Civil Engineering*, 2017. 21(4): p. 1273-1281.
13. Chai, H., A.A. Majeed, and A.A. Allawi, Torsional analysis of multicell concrete box girders strengthened with CFRP using a modified softened truss model. *Journal of Bridge Engineering*, 2015. 20(8): p. B4014001.
14. Tais, A. and M. Abdulrahman, Improving The Torsional Strength of Reinforced Concrete Hollow Beams Strengthened with Externally Bonded Reinforcement CFRP Stripe Subjected to Monotonic and Repeated Loads. *Information Sciences Letters*, 2023. 12(1): p. 427-441.
15. Alabdulhady, M.Y., L.H. Sneed, and C. Carloni, Torsional behavior of RC beams strengthened with PBO-FRCM composite—An experimental study. *Engineering Structures*, 2017. 136: p. 393-405.
16. ACI, ACI 318-14. Building code requirements for structural concrete. 2014, ACI Farmington Hills, MI, USA.
17. Designation, A., C370-05a,(2005)" Standard Specification for Testing Method and Definitions for Mechanical Testing of Steel Products. 2005 Annual Book of ASTM Standards, American Society for Testing and Material, Philadelphia, Pennsylvania, Section. 1: p. 248-287.
18. ASTM, A., ASTM C39/C39M-18 standard test method for compressive strength of cylindrical concrete specimens. ASTM International, West Conshohocken, PA. ASTM, AI (2018)." ASTM C, 2018. 192.
19. ASTM, C., 496/C496M-11. Standard Test Method for Splitting Tensile Strength of Cylindrical Concrete, ASTM, West Conshohocken, PA, 2011. 5.
20. ASTM, A., C78/C78M, ASTM C78/C78M-02-standard test method for flexural strength of

- concrete (using simple beam with third-point loading). ASTM Int., 2002.
21. Astm, C., 496/C 496M. Standard Test Method for Splitting Tensile Strength of Cylindrical Concrete Specimens,” ASTM International, West Conshohocken, PA, 2004.
  22. Panchacharam, S. and A. Belarbi. Torsional behavior of reinforced concrete beams strengthened with FRP composites. in First FIB Congress, Osaka, Japan. 2002.
  23. Aljazaeri, Z.R. and J.J. Myers, Fatigue and flexural behavior of reinforced-concrete beams strengthened with fiber-reinforced cementitious matrix. *Journal of Composites for Construction*, 2017. 21(1): p. 04016075.
  24. Peng, X.-N. and Y.-L. Wong, Behavior of reinforced concrete walls subjected to monotonic pure torsion—An experimental study. *Engineering structures*, 2011. 33(9): p. 2495-2508.